

Numerical Solution of an Etching Problem

C. VUIK*

Philips Research Laboratories, P.O. Box 80.000, 5600 JA Eindhoven, The Netherlands

AND

C. CUVELIER

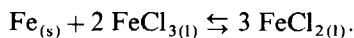
*Delft University of Technology, Department of Mathematics and Informatics,
Delft, The Netherlands*

Received September 16, 1983; revised February 13, 1984

After a short description of the chemical background of etching processes, a simplified mathematical model is formulated. This contains two parameters that determine the etching profile. Two approaches for obtaining a numerical solution are discussed. First, the problem in terms of a variational inequality is reformulated and some new results on its numerical solution are presented. Then, how the problem can be solved by means of a moving grid method as well is explored. Results obtained by both methods are presented and compared. The latter method is applicable to a much wider class of boundary conditions, but the variational inequality approach seems attractive for other reasons. Finally this work is compared with some experimental results. © 1985 Academic Press, Inc.

I. INTRODUCTION

Wet chemical etching is an important technique in modern technology as can be exemplified by the production of oil filters, masks for colour TV sets and integrated circuits. A typical case is the etching of Fe with FeCl_3 , whose chemical reaction at the interface is given by



Another example is the etching of SiO_2 by HF solutions buffered with NH_4F . This process is important in the manufacturing of micro-electronic devices.

In this paper the shape of the etching profile is investigated numerically. In practice the following features of the etching profile are important. First, there is the phenomenon of undercutting, by which we understand the etching of the sidewalls below the photoresist layer (see [1, 2]). In the production of integrated circuits, undercutting could result in short-circuit and other inaccuracies. Further, at contact

* Present address: University Utrecht, Department of Mathematics, Utrecht, The Netherlands.

windows a tapered profile at the edge of the window is required. A sharp step at the edge is a source of many failures of integrated circuits (see [3]). In the mathematical model, parameters related to the etching profile can easily be varied. By solving the etching problem the influence of these parameters can be investigated. Combined with experiments, this model can be a useful tool to predict and understand the etching profile. For more details concerning the numerical solution of the etching problem we refer to [4].

II. MATHEMATICAL MODEL

We define the following problem. A gap of width $2a$ and length L is to be etched in a flat plate. The remainder of the plate is covered with a protective (photoresist) layer. Since we assume that L is much larger than $2a$, the problem can be considered as two dimensional (see Fig. 1).

We make the following assumptions. There is no convection in the etching medium; the etching process is isotropic; the thickness of the photoresist layer is infinitely small and only one component of the etching liquid determines the process. In the region $\Omega(t)$ the concentration $C(\text{mol}/\text{m}^3)$ of the component satisfies the diffusion equation

$$\frac{\partial C}{\partial t} - \mathbf{D} \Delta C = 0 \quad \text{in } \Omega(t). \tag{2.1}$$

$\mathbf{D}(\text{m}^2/\text{sec})$ is the diffusion coefficient (see [5]). Since there is no mass transfer through the photoresist layer $\Gamma_2(t)$, the boundary condition is given by

$$\frac{\partial C}{\partial \bar{n}} = 0 \quad \text{on } \Gamma_2(t) \tag{2.2}$$

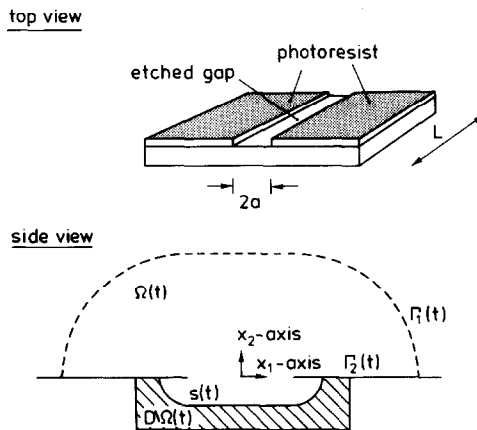


FIG. 1. The etching fluid $\Omega(t)$ is bounded by the outer boundary Γ_1 , the photoresist layer $\Gamma_2(t)$, and the moving boundary $S(t)$. $D \setminus \Omega(t)$ denotes part of the solid.

where \bar{n} denotes the unit normal vector on $\Gamma_2(t)$ pointing outward with respect to $\Omega(t)$. At Γ_1 the concentration is set equal to C_0 . Typical of this problem is that part of the boundary is moving with respect to time. The mass balance at the moving boundary $S(t)$ yields the boundary condition

$$v_n = -\sigma \frac{\partial C}{\partial \bar{n}} \quad \text{on } S(t). \quad (2.3)$$

v_n can be interpreted as the normal velocity of the boundary $S(t)$ and the parameter σ ($\text{m}^2/\text{sec}/\text{mol}$) is a material constant. Another condition on the moving boundary is obtained by the fact that the rate of reaction must equal the rate of diffusion. For a first-order reaction like the one considered here this leads to the boundary condition (see [6])

$$\mathbf{D} \frac{\partial C}{\partial \bar{n}} = -kC \quad \text{on } S(t) \quad (2.4)$$

where k (m/sec) denotes the rate of reaction. When k is large with respect to \mathbf{D}/a the boundary condition (2.4) can be replaced by

$$C = 0 \quad \text{on } S(t). \quad (2.5)$$

The initial conditions for C are given by

$$C = C_0 \quad \text{in } \Omega(t=0). \quad (2.6)$$

We introduce the following characteristic quantities: length scale a , concentration scale C_0 , and time scale a^2/\mathbf{D} . In dimensionless form the problem is to find a function $C = C(x, t)$, $x \in \Omega(t)$, $t \in [0, T]$ and a boundary $S(t)$, $t \in [0, T]$ such that

$$\frac{\partial C}{\partial t} - \Delta C = 0 \quad \text{in } Q_\Omega = \{(x, t) \mid x \in \Omega(t), t \in (0, T)\} \quad (2.7)$$

together with the initial condition

$$C = 1 \quad \text{in } \Omega(t=0) \quad (2.8)$$

and boundary conditions

$$C = 1 \quad \text{on } \Gamma_{1t} = \Gamma_1 \times (0, T), \quad (2.9)$$

$$\frac{\partial C}{\partial \bar{n}} = 0 \quad \text{on } \Gamma_{2t} = \{(x, t) \mid x \in \Gamma_2(t), t \in (0, T)\}. \quad (2.10)$$

The conditions on the moving boundary $S(t)$ give rise to two different models: If k tends to infinity,

$$\left. \begin{aligned} C &= 0 \\ \frac{\partial C}{\partial \bar{n}} &= -Bv_n \end{aligned} \right\} \text{ on } S_t = \{(x, t) \mid x \in S(t), t \in (0, T)\}, \tag{2.11}$$

$$\tag{2.12}$$

whereas for finite k ,

$$\left. \begin{aligned} \frac{\partial C}{\partial \bar{n}} &= -ShC \\ \frac{\partial C}{\partial \bar{n}} &= -Bv_n \end{aligned} \right\} \text{ on } S_t. \tag{2.13}$$

$$\tag{2.14}$$

In this formulation there appear two dimensionless groups. The first one is $B = \mathbf{D}/\sigma C_0$ and the second one, called the Sherwood number, is defined by $Sh = ak/\mathbf{D}$.

The magnitude of Sh indicates which model is to be considered. For large Sh the problem is diffusion-controlled, whereas for small Sh the problem is activation-controlled. Both models can occur in practice. Similar diffusion problems are encountered in crystal growth theory (see [7]). The above-stated problem is a so-called moving boundary problem. After [8], we define free boundary problems to be boundary value problems involving (partial) differential equations on domains, part of whose boundaries must be determined as part of the solution. A moving boundary problem is defined to be an initial-value problem for (partial) differential equations involving free boundaries. For those who are interested in a general account of the mathematical methods applicable to free and moving boundary problems as well as their physical background, we refer to [9, 10].

III. METHOD OF VARIATIONAL INEQUALITIES

The method of variational inequalities will be applied to problem (2.7)–(2.12). More generally the conditions (2.8)–(2.10) are replaced by $C = C_0$ in $\Omega(t=0)$ and $C = g$ on $\Gamma_t = \Gamma_{1t} \cup \Gamma_{2t}$, respectively. The functions $g = g(x, t)$ and $C_0 = C_0(x)$ are nonnegative, while B is a strictly positive constant.

Note that, since on the one hand C vanishes on S_t and on the other hand C is nonnegative in Q_Ω , the normal derivative of C is nonpositive on S_t , which implies that $\Omega(t)$ is a nondecreasing set with respect to t . In this respect the formulation of the etching problem is equivalent to the one-phase Stefan problem. The main difficulty in solving this problem is of course to satisfy the two interface conditions on the moving boundary S_t . A technique which avoids this difficulty and which eliminates in some sense the moving boundary S_t is to formulate the problem as a variational inequality. As we shall see, this has two major advantages:

(i) A formulation in terms of a variational inequality leads in a simple way to existence and uniqueness theorems.

(ii) The formulation suggests an efficient numerical method for which stability and convergence can be proved.

We assume that D is chosen large enough so as to contain strictly $\Omega(t)$ for all $t \in (0, T)$. To formulate the etching problem as a variational inequality let us define an extension \hat{C} of C to the whole domain $Q_D = D \times (0, T)$ by

$$\hat{C}(x, t) = \begin{cases} C(x, t) & \text{in } Q_\Omega \\ 0 & \text{in } Q_D \setminus Q_\Omega \end{cases}$$

and, accordingly,

$$\hat{g}(x, t) = \begin{cases} g(x, t) & \text{on } \Gamma_t \\ 0 & \text{on } (\partial D \times (0, T)) \setminus \Gamma_t \end{cases}$$

$$\hat{C}_0(x) = \begin{cases} C_0(x) & \text{in } \Omega(t=0) \\ 0 & \text{in } D \setminus \Omega(t=0). \end{cases}$$

Next we define χ_Ω as the characteristic function of Q_Ω in Q_D . It can be shown (see [11]) that \hat{C} satisfies

$$\frac{\partial \hat{C}}{\partial t} - \Delta \hat{C} = -B \frac{\partial \chi_\Omega}{\partial t} \quad \text{in } Q_D \tag{3.1}$$

$$\hat{C} = \hat{g} \quad \text{on } \partial D \times (0, T) \tag{3.2}$$

$$\hat{C} = \hat{C}_0 \quad \text{in } D, \quad t = 0 \tag{3.3}$$

in a distributional sense.

Following [12] and [13], we introduce the following dependent variable,

$$u(x, t) = \int_0^t \hat{C}(x, \tau) \, d\tau \quad x \in D, \quad t \in (0, T). \tag{3.4}$$

By integrating equation (3.1) with respect to t , we obtain

$$\frac{\partial u}{\partial t} - \Delta u = f + B(1 - \chi_\Omega) \tag{3.5}$$

with $f(x) = \hat{C}_0(x) - B(1 - \chi_\Omega(x, 0))$, f independent of time.

It is easy to verify that u solves the following problem:

$$\left. \begin{aligned} \frac{\partial u}{\partial t} - \Delta u - f &\geq 0 \\ u &\geq 0 \\ \left(\frac{\partial u}{\partial t} - \Delta u - f \right) u &= 0 \end{aligned} \right\} \quad \text{in } Q_D \tag{3.6}$$

$$\begin{aligned}
 u(x, t) &= \int_0^t \hat{g}(x, \tau) \, d\tau = G(t) && \text{on } \partial D \times (0, T) \\
 u &= 0 && \text{in } D, t = 0.
 \end{aligned}$$

It is immediately verified that, reciprocally, if u is a solution of (3.6), then $\hat{C} = \partial u / \partial t$ is a solution of the original problem (3.1), (3.2), and (3.3).

To prove existence and uniqueness of a solution of problem (3.6) we introduce some function spaces: $L_2(D)$ denotes the Hilbert space of square-integrable functions on D with inner product

$$(v, w)_0 = \int_D v \cdot w \, dx \quad v, w \in L_2(D).$$

The space $H^1(D)$ is the Sobolev space of functions on D which belong to $L_2(D)$ as well as their first derivatives. The inner product in $H^1(D)$ is

$$(v, w)_1 = (v, w)_0 + (\nabla v, \nabla w)_0 \quad v, w \in H^1(D).$$

Finally we define a closed convex nonempty subset $K(t)$ of $H^1(D)$ by

$$K(t) = \{v \in H^1(D) \mid v \geq 0, v = G(t) \text{ in the trace sense on } \partial D\}.$$

From (3.6) we deduce easily that $u(x, t)$ satisfies formally

$$\left(\frac{\partial u}{\partial t}, v - u \right)_0 + (\nabla u, \nabla(v - u))_0 - (f, v - u)_0 \geq 0 \quad \forall v \in K(t), \quad u(t) \in K(t) \quad (3.7)$$

$$u(0) = 0. \quad (3.8)$$

An element $u \in L_2(0, T; H^1(D))$ with $\partial u / \partial t \in L_2(0, T; L_2(D))$ is called a strong solution of the etching problem if u satisfies (3.7) together with (3.8). Here we denote by $L_2(0, T; H)$ generally the space of L_2 -integrable functions on $(0, T)$ with values in H . The following theorem is proved in [14]:

THEOREM 3.1. *Let $\hat{C}_0 \in L_2(D)$ and $G \in L_2(0, T; H^{1/2}(\partial D))$, then there exists a unique strong solution of the etching problem. The moving boundary is the interface separating the regions*

$$\{(x, t) \in Q_D \mid u(x, t) > 0\} \quad \text{and} \quad \{(x, t) \in Q_D \mid u(x, t) = 0\}.$$

In the remainder of this section we shall discuss how to solve the parabolic variational inequality (3.7), (3.8) using a finite element method. To do so we assume that D is a polygonal region in \mathbb{R}^2 . Then we cover D by a union of non-degenerate triangles T with diameters less than or equal to h . With respect to time we use a finite difference method with step $\Delta T = T/N$, where N is a sufficiently large integer number.

Let V_h denote the finite element approximation of $H^1(D)$ defined as the space of continuous functions which are affine on each triangle T . The set $K(t)$ is discretized as

$$K_h^n = \{v_h \in V_h \mid v_h \geq 0, v_h|_{\partial D} = G_h(n \cdot \Delta T)\}$$

where the function G_h denotes an approximation of G which is piecewise continuous on D and affine on each nonempty intersection $T \cap \partial D$. We introduce the following notations:

$$u_h^n = u_h(n \cdot \Delta T) \quad u_h^{n+\theta} = \theta u_h^{n+1} + (1-\theta) u_h^n \quad 0 \leq \theta \leq 1$$

$$u_h(t) = \frac{(n+1)\Delta T - t}{\Delta T} u_h^n + \frac{t - n \cdot \Delta T}{\Delta T} \cdot u_h^{n+1} \quad \text{on } [n \cdot \Delta T, (n+1) \cdot \Delta T]$$

The finite element analogue of (3.7), (3.8) is formulated as follows:

Let $u_h^0 = 0$.

Then for $n = 0, 1, \dots, N-1$, find $u_h^{n+1} \in K_h^{n+1}$ such that

$$\left(\frac{u_h^{n+1} - u_h^n}{\Delta T}, v_h - u_h^{n+1} \right)_0 + (\nabla u_h^{n+\theta}, \nabla (v_h - u_h^{n+1}))_0 \geq (f, v_h - u_h^{n+1})_0 \quad \forall v_h \in K_h^{n+1}. \tag{3.9}$$

The following theorem can be deduced from [9]:

THEOREM 3.2. (i) *There exists a unique solution u_h^{n+1} , $n = 0, 1, \dots, N-1$ of (3.9).*

(ii) *The solution u_h^n , $n = 0, \dots, N$ of (3.9) is stable in the sense that*

$$\|u_h^n\|_0^2 + \sum_{l=1}^N \|\nabla u_h^l\|_0^2 \leq \gamma \quad \gamma \text{ independent of } h \text{ and } \Delta T$$

provided

$$(1 - 2\theta) \cdot \Delta T (S(h))^2 < 2 \quad \text{for } 0 \leq \theta < \frac{1}{2} \tag{3.10}$$

where $S(h) = 3/2 \cdot h \cdot \max_T 1/|T|$, $|T|$ is the area of T .

(iii) *When $(\Delta T, h) \rightarrow (0, 0)$ in such a way that condition (3.10) is satisfied and*

$$(1 - \theta) \cdot \Delta T \cdot (S(h))^2 \quad \text{bounded} \tag{3.11}$$

then $u_h \rightarrow u$ weakly in $L_2(0, T; H^1(D))$.

For the actual computation of u_h^{n+1} we shall write problem (3.9) in another form. For this we remark that to every element $v_h \in V_h$ there corresponds a vector \bar{v}_h whose components are just the values of v_h in the nodal points. Thus $\bar{v}_h = (v_{h1}, \dots, v_{hM})$, where M is the number of nodal points and $v_{hj} = v_h(x_j)$, x_j being

the j th nodal point. \bar{K}_h^n is the set of M -dimensional vectors whose components are nonnegative and which satisfy $v_{hj} = G_h(x_j, n \Delta T)$ when $x_j \in \partial D$. Furthermore we define a matrix A_h and a vector \bar{b}_h^n by

$$\bar{v}_h^T A_h \bar{w}_h = \frac{1}{\Delta T} (v_h, w_h)_0 + \theta (\nabla v_h, \nabla w_h)_0, \quad \forall v_h, w_h \in V_h,$$

$$(\bar{b}_h^n)^T \bar{w}_h = (f, w_h)_0 + \frac{1}{\Delta T} (u_h^n, w_h)_0 + (\theta - 1) (\nabla u_h^n, \nabla w_h)_0, \quad \forall w_h \in V_h,$$

then problem (3.9) can be written as

$$\begin{aligned} &\text{find } \bar{u}_h^{n+1} \in \bar{K}_h^{n+1} \text{ such that} \\ J_h(\bar{u}_h^{n+1}) = \inf_{\bar{v}_h \in \bar{K}_h^{n+1}} J(\bar{v}_h), \quad J(\bar{v}_h) = \frac{1}{2} \bar{v}_h^T A_h \bar{v}_h - (\bar{b}_h^n)^T \bar{v}_h \end{aligned} \tag{3.12}$$

or, equivalently,

$$\begin{aligned} &\text{find } \bar{x}_h = \bar{u}_h^{n+1} \in \bar{K}_h^{n+1} \text{ such that} \\ A_h \bar{x}_h - \bar{b}_h^n \geq 0; \quad (\bar{x}_h)^T (A_h \bar{x}_h - \bar{b}_h^n) = 0. \end{aligned} \tag{3.13}$$

This quadratic programming problem will be solved by the method of successive overrelaxation with projection [15, 16] which can be considered as a generalization of the classical Gauss-Seidel algorithm. Let $\bar{x}_h^0 \in \bar{K}_h^{n+1}$, then we define the sequence $\bar{x}_h^{(1)}, \bar{x}_h^{(2)}, \dots, \bar{x}_h^{(m)}, \dots$, of elements in \bar{K}_h^{n+1} by

$$\begin{aligned} \bar{x}_{hi}^{(m+1/2)} &= -\frac{1}{(A_h)_{ii}} \left\{ \sum_{j=1}^{i-1} (A_h)_{ij} \bar{x}_{hj}^{(m+1)} + \sum_{j=i+1}^M (A_h)_{ij} \bar{x}_{hj}^{(m)} - \bar{b}_{hi}^n \right\} \\ \bar{x}_{hi}^{(m+1)} &= \max \{ 0, (1 - \omega) \bar{x}_{hi}^{(m)} + \omega \bar{x}_{hi}^{(m+1/2)} \} \end{aligned} \tag{3.14}$$

where ω is called the relaxation parameter. Since the matrix A_h is symmetric and positive definite, the following result concerning the convergence of the sequence $\{\bar{x}_h^{(m)}\}_{m=0,1,2,\dots}$ can be proved [15, 16].

THEOREM 3.3. *For any ω satisfying $0 < \omega < 2$, the sequence $\{\bar{x}_h^{(m)}\}_{m=0,1,2,\dots}$ defined by (3.14) converges to the solution \bar{x}_h of problem (3.13).*

A natural choice for the initial guess \bar{x}_h^0 of the solution \bar{x}_h is of course the solution of the preceding time step, thus $\bar{x}_h^{(0)} = u_h^n$. Another question that arises is whether there is a value of ω such that the rate of convergence is optimized. When the classical successive overrelaxation method is applied to solve a system of linear equations $\bar{A}_h \bar{x}_h = \bar{b}_h$, where \bar{A}_h is symmetric, positive definite and 2-cyclic consistently ordered, the optimal relaxation parameter $\tilde{\omega}_{\text{opt}}$ is known in terms of the spectral radius $\tilde{\mu}$ of the Gauss-Seidel GS(\bar{A}_h) matrix corresponding to \bar{A}_h [17]

$$\tilde{\omega}_{\text{opt}} = \frac{2}{1 + (1 - \tilde{\mu})^{1/2}}$$

When a similar analysis is applied to the successive overrelaxation method with projection, the following results can be obtained [15, 16] (see also [4]). Let us denote by $I(\bar{x}_h^{(m)})$ a subset of $\{1, 2, \dots, M\}$ defined by the relation

$$j \in I(\bar{x}_h^{(m)}) \Leftrightarrow x_{hj}^{(m)} > 0.$$

Then it can be proved that there exists an integer m_0 such that

$$I(\bar{x}_h^{(m)}) = I(\bar{x}_h) \quad \text{for all } m > m_0.$$

Next we define by $A_h(I(\bar{x}_h))$ the submatrix of A_h obtained by deleting those elements $(A_h)_{ij}$ for which $i \notin I(\bar{x}_h)$ or $j \notin I(\bar{x}_h)$. Now it can be proved that if $I(\bar{x}_h) \neq \emptyset$, x_{hj} and $(A_h \bar{x}_h - \bar{b}_h^n)_j$ do not vanish simultaneously and $\Omega(t)$ is a simply connected domain, then the optimal value of ω is given by

$$\omega_{\text{opt}} = \frac{2}{1 + (1 - \mu)^{1/2}}, \tag{3.15}$$

where μ denotes the spectral radius of $\text{GS}(A_h(I(\bar{x}_h)))$. Since, in general, neither $I(\bar{x}_h)$ nor μ is known explicitly we use the following estimate for ω_{opt} , which has proved to be very accurate in practice. First, we set $\omega = 1$ and we calculate $\bar{x}_h^{(1)}, \dots, \bar{x}_h^{(m_0+2)}$, where it was found that $M^{1/2}$ is a good approximation of m_0 . An estimate of the spectral radius of $\text{GS}(A_h(I(\bar{x}_h)))$ is given by (cf. [18])

$$\mu^* = q^{(m_0+2)}/q^{(m_0+1)}; \quad q^{(m)} = \sum_{j=1}^M |\bar{x}_j^{(m)} - \bar{x}_j^{(m-1)}|, \quad m = 1, 2, \dots$$

According to relation (3.15) we estimate ω_{opt} by

$$\omega^* = \frac{2}{1 + (1 - \mu^*)^{1/2}}.$$

Next we perform again m_0 iterations with $\omega = 1 + 2/3(\omega^* - 1)$. This value was chosen since for the computation of a more accurate estimate of μ , the relaxation parameter is preferably underestimated instead of overestimated [17, 18]. Setting now

$$\lambda = q^{(2m_0+2)}/q^{(2m_0+1)}$$

we use the following estimate of the spectral radius of $\text{GS}(A_h(I(\bar{x}_h)))$ ([17, 18]),

$$\mu^{**} = \frac{1}{\lambda} \left(\frac{\lambda - 1 + \omega}{\omega} \right)^2 \quad \omega = 1 + 2/3(\omega^* - 1)$$

hence using (3.15),

$$\omega^{**} = \frac{2}{1 + (1 - \mu^{**})^{1/2}},$$

Finally, ω_{opt} will be slightly overestimated by taking

$$\omega_{\text{opt}} = 2 + 4/5(\omega^{**} - 2). \quad (3.16)$$

Since it can be proved that on $S(t)$ both u and $\partial u / \partial \bar{n}$ are zero, the approximate free boundary was determined by an interpolation procedure based on the quadratic form of u near $S(t)$ [4, 9].

IV. MOVING GRID METHOD

In Section III the etching problem was solved for infinite Sherwood number using the theory of variational inequalities. It seems to be impossible to construct a variational formulation for finite Sh . To solve problem (2.7)–(2.10), (2.13), (2.14) for finite Sh we shall use a moving grid method (see [19–21]) based on a finite element discretization of the problem in the space variables and a finite difference discretization in the time variable. The moving grid method is based on the following principle. The solution C at time $t = (n + 1) \Delta T$ is calculated by solving the discretized problem (2.7)–(2.10), (2.13) in the region $\Omega(n \cdot \Delta T)$ bounded by Γ_1 , $\Gamma_2(n \Delta T)$ and $S(n \cdot \Delta T)$. Next the free boundary $S((n + 1) \cdot \Delta T)$ is calculated by moving the boundary $S(n \cdot \Delta T)$ according to the discrete analogue of (2.14). This procedure is repeated for $n = 0, 1, \dots, N - 1$; note that $S(t = 0)$ is known. This moving grid method is also applicable for infinite Sherwood number, and this allows us, for $Sh \rightarrow \infty$, to compare the results obtained using the variational inequality approach with those obtained with the moving grid method. At each time step the finite element grid is adapted to ensure that the location of the moving boundary coincides with nodal points. The effect of the deforming grid is reflected by an extra (convective) term in the diffusion equation. Suppose that at time $t = n \cdot \Delta T$ the nodal points are given by x_j^n , $j = 1, 2, \dots, M$, then the discrete backward time derivative of C at time $(n + 1) \Delta T$ in the nodal point x_j^{n+1} is given by

$$\frac{\partial C^{n+1}}{\partial t}(x_j^{n+1}) = \frac{C^{n+1}(x_j^{n+1}) - C^n(x_j^{n+1})}{\Delta T} \quad (4.1)$$

Since, in general, x_j^{n+1} is not a nodal point of the triangulation at time $t = n \cdot \Delta T$, the value of C^n at x_j^{n+1} must be obtained by linear interpolation

$$C^n(x_j^{n+1}) = C^n(x_j^n) + \delta x_j^n \cdot \nabla C^n(x_j^n), \quad (4.2)$$

where $\delta x_j^n = x_j^{n+1} - x_j^n$; and where it is assumed that x_j^n is close to x_j^{n+1} . Substitution of (4.2) into (4.1) gives

$$\frac{\partial C^{n+1}}{\partial t}(x_j^{n+1}) = \frac{C^{n+1}(x_j^{n+1}) - C^n(x_j^n)}{\Delta T} - \frac{\delta x_j^n}{\Delta T} \nabla C^n(x_j^n). \quad (4.3)$$

The time discretization of (2.8) can now be written as

$$\frac{C^{n+1}(x_j^{n+1}) - C^n(x_j^n)}{\Delta T} - \Delta C^{n+1}(x_j^{n+1}) = \frac{\delta x_j^n}{\Delta T} \nabla C^n(x_j^n). \tag{4.4}$$

In the application of the finite element method to the etching problem, the domain above the photoresist layer is covered by triangles which do not vary in time. The remainder of $\Omega(t)$ is subdivided into triangles which are adapted at each time step (see Fig. 2).

For small values of t there is a difficulty because the triangles below the x_1 axis are nearly degenerate. The angle condition [22], however, assures stability. Setting

$$f^n = C_h^n + \frac{\delta x}{\Delta T} \cdot \nabla C_h^n$$

the finite element formulation corresponding to (4.4) reads

for $n = 0, 1, \dots, N$, find $C_h^{n+1} \in V_h^n$ such that

$$\frac{1}{\Delta T} (C_h^{n+1}, v_h) + (\nabla C_h^{n+1}, \nabla v_h) + Sh \int_{S(n\Delta T)} C_h^{n+1} v_h \, ds = (f^n, v_h), \tag{4.5}$$

$$\forall v_h \in V_{h0}^n, \quad C_h^0 = C_{0h}$$

where $(v, w) = \int_{\Omega(t)} v \cdot w \, d\Omega$ and V_h^n denotes a subset of the finite element approximation of $H^1(\Omega(n \cdot \Delta T))$ consisting of functions which are continuous on

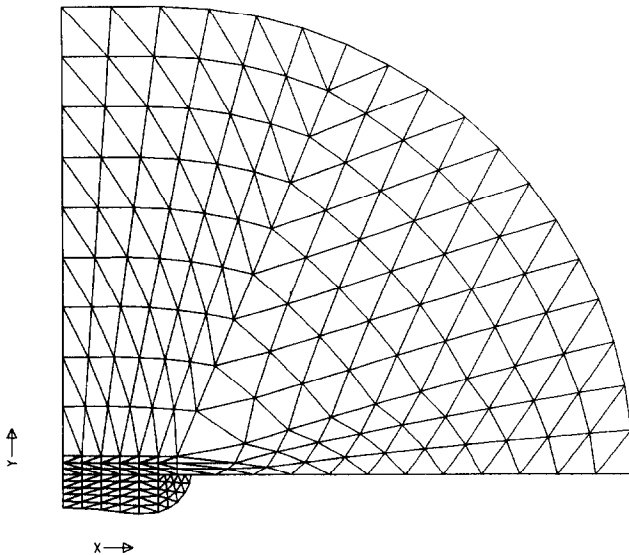


FIG. 2. The grid used in the moving grid method.

$\Omega(n \cdot \Delta T)$, affine on each element and which satisfy the discrete analogue of (2.9). The space V_{h0}^n is similar to V_h^n but consists of functions which vanish on Γ_1 . As the stiffness matrix and the right-hand vector corresponding to (4.5) change at each time step, it is preferable to apply an iterative solution method rather than a direct one.

Once the solution C_h^{n+1} has been calculated, we can use (2.14) to determine the new position of the free boundary. An explicit form of (2.14) is given by [21, 23]

$$\nabla C_h^{n+1} \cdot \bar{n} = -B \frac{s^{n+1} - s^n}{\Delta T} \cdot \bar{n}, \tag{4.6}$$

where $s^n = (s_1^n, s_2^n)$ denotes the position of the free boundary at time $n \cdot \Delta T$ and the vector $s^{n+1} - s^n$ points in the normal direction. Equation (4.6) can be written as

$$s^{n+1} = s^n - \frac{\Delta T}{B} (\nabla C_h^{n+1} \cdot \bar{n}) \bar{n}. \tag{4.7}$$

It can be proved [21] that scheme (4.5), (4.7) remains stable in internal nodes, but that for large ΔT instabilities in the solution can occur in the vicinity of the moving boundary.

For large Sherwood numbers, the gradient of C_h^{n+1} at the moving boundary is approximately pointing in the normal direction. In this case (4.7) can be replaced by

$$s^{n+1} = s^n - \frac{\Delta T}{B} \nabla C_h^{n+1}. \tag{4.8}$$

However, for small Sherwood numbers, the gradient of C_h^{n+1} at the moving boundary has a nonvanishing component in the tangential direction. Now we determine points $s_j^{n+1/2}$ with Eq. (4.8). The intersection of the line through the points $s_{j-1}^{n+1/2}$,

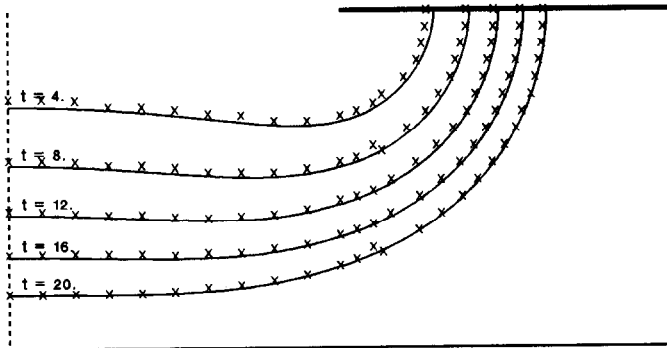


FIG.3. The moving boundary plotted for $B=10$ and $Sh=1000$. The solid line is computed with method 2, whereas the crosses represent the solution by method 1.

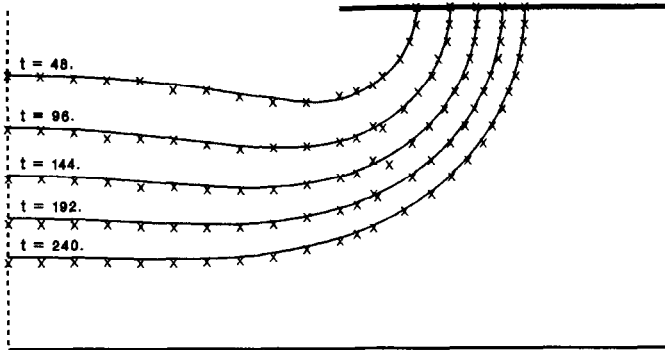


FIG. 4. The moving boundary plotted for $B=100$ and $Sh=1000$. The solid line is computed with method 2, whereas the crosses represent the solution by method 1.

$s_{j+1}^{n+1/2}$ with the line through s_j^n pointing in the normal direction, is a good approximation of the free boundary point s_j^{n+1} defined by Eq. (4.7).

Since the domain $\Omega(t)$ is expanding in time, the finite element triangulation becomes coarser and coarser. When the grid size exceeds a certain limit the triangulation is replaced by a finer one. The solution C_h^n on the finer grid is obtained from the solution C_h^n on the coarser grid by linear interpolation. The interpolation error introduced in this way is of the same order as the discretization error.

V. RESULTS AND CONCLUSIONS

The numerical method of solving the variational inequality—stated in Section III—has been evaluated for model problems whose exact solution is known. It

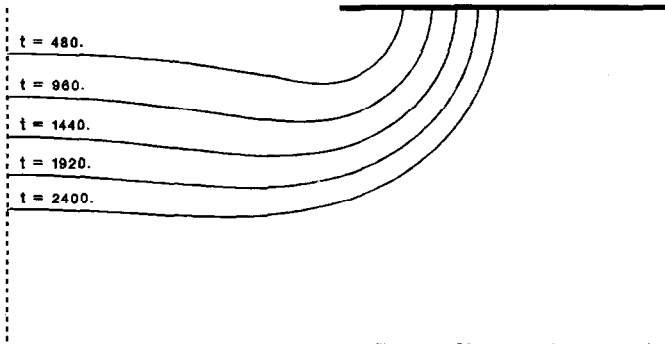


FIG. 5. The moving boundary computed with method 2 is plotted for $B=1000$ and $Sh=1000$.

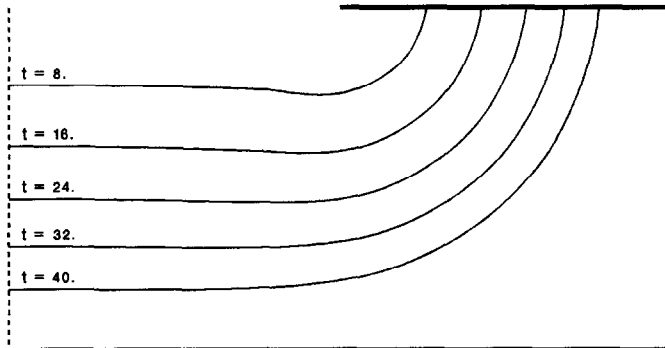


FIG. 6. The moving boundary computed with method 2 is plotted for $B=10$ and $Sh=1$.

appears that the estimated ω speeds up the convergence considerably. In a one-dimensional problem Cryer's estimation of ω requires 31 iterations, whereas for our estimation 12 iterations are sufficient to obtain the same accuracy. After the solution is computed, the location of the moving boundary can be approximated by the nodal points, where the solution becomes zero. This requires a refined grid to locate the boundary with sufficient accuracy. With the parabolic interpolation mentioned in Section III the accuracy of the boundary estimation is much better. This is verified for model problems and follows easily from the Figs. 3 and 4, because the distance between the two solutions is small with respect to the radius of the triangles. The geometry of the problem is depicted in Fig. 1. Since the problem is symmetric with respect to the x_2 axis, it is solved in the half space $x_1 \geq 0$. The photoresist layer is represented by a line at the x_1 axis. The outer boundary Γ_1 is chosen in such a way, that the concentration C at Γ_1 can be considered as nearly constant ($C=1$). To avoid that for large values of the time t (or large values of B),

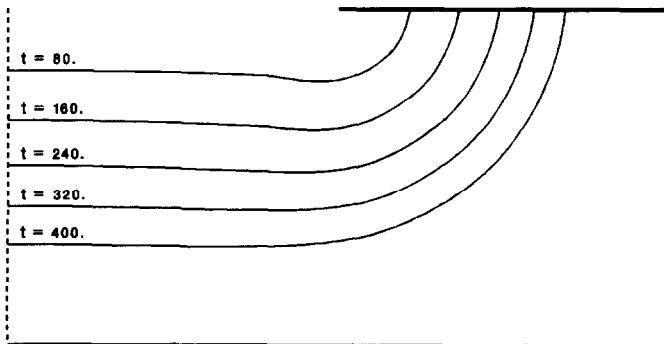


FIG. 7. The moving boundary computed with method 2 is plotted for $B=100$ and $Sh=1$.

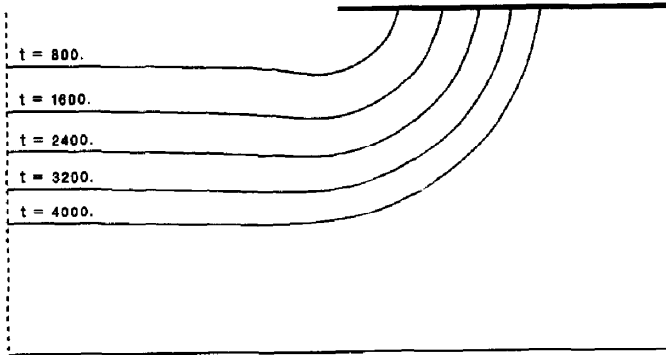


FIG. 8. The moving boundary computed with method 2 is plotted for $B = 1000$ and $Sh = 1$.

the boundary Γ_1 is too far away from the gap, which would enlarge the computational work, the following asymptotic solution (cf. [24]) can be used:

$$C(x_1, x_2, t) = 1 - \frac{1}{2\pi} \int_0^t \exp\left(\frac{-(x_1^2 + x_2^2)}{4\tau}\right) \left(\int_{-1}^1 \frac{\partial C(\xi, 0, t - \tau)}{\partial y} d\xi \right) d\tau$$

for $x_2 \geq 0$ and $x_1^2 + x_2^2 \gg 1$. Using this approximation in our numerical scheme enables us to compute the solution for very large values of B .

In Figs. 3-5 the etching profile is plotted. The solutions obtained by the variational inequality method (method 1) and the moving grid solution (method 2) show good correspondence. Method 1 is applied with $\theta = 0.5$. The time interval is divided equidistantly into a hundred time steps; the domain D is discretized with 1291 grid points. There are no instabilities observed. The numerical problem is solved by the overrelaxation method with projection. After every ten time steps ω_{opt} is approximated. With method 2 the time interval is also divided into a hundred time steps. Since $\Omega(t)$ increases with time the number of nodal points also increases

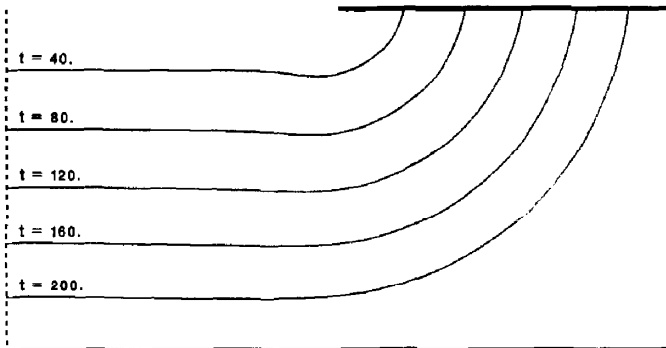


FIG. 9. The moving boundary computed with method 2 is plotted for $B = 10$ and $Sh = 0.1$.

from 169 at $t=0$ to 379 at $t=T$. In this method the linear equations are solved with a conjugate gradient method.

For short times the profiles in Figs. 3–5 are deeper at the edge of the photoresist than at the middle of the gap. This agrees well with some results obtained in experiments at our laboratories. Later on this bulge disappears, whereas for large times the profiles tend to an ellipse [24]. The angle of the profile with the photoresist layer is 90 degrees.

In Figs. 6–8 the solution is shown for $Sh = 1$. The bulge in the profile disappears for small values of Sh . The angle between the tangent at the profile and the photoresist layer is smaller than the corresponding angle for large values of Sh at the same etching depth.

In Fig. 9 the solution is plotted for $Sh = 0.1$. The spacing between successive profiles becomes nearly equidistant. For $Sh \ll 1$ the problem is activation-controlled. In this case the normal velocity of the moving boundary is constant in place and time. This is in accordance with the results plotted in Fig. 9.

After comparison of the two methods the following conclusions can be drawn. Method 1 has a firm mathematical basis. In general, method 1 requires less computing time than method 2, for the same accuracy. When there are several moving boundaries, or when the moving boundary meets a rigid wall, method 2 requires complicated programming, whereas method 1 is still easy to implement. A disadvantage, however, is that for certain problems it is not easy, and perhaps impossible, to formulate a variational inequality, so method 2 has a wider range of applicability.

ACKNOWLEDGMENTS

We thank J. de Groot for stimulating discussions and valuable suggestions concerning this work. We also thank H. K. Kuiken for suggesting the problem.

Note added in proof. Actually as we shall show in a following paper formulas (2.13) and (2.14) are a kind of first-order approximations (for B and/or Sh large). In full generality the mass balance at the moving boundary yields

$$\frac{\partial C}{\partial \bar{n}} + Cv_n = -ShC \quad \text{on } S_t$$

$$\frac{\partial C}{\partial \bar{n}} + Cv_n = -Bv_n \quad \text{on } S_t.$$

Formulas (2.11), (2.12) remain the same.

REFERENCES

1. D. M. ALLEN, D. F. HORNE, AND G. W. W. STEVENS, *J. Photogr. Sci.* **25** (1977), 254.
2. D. M. ALLEN, D. F. HORNE, AND G. W. W. STEVENS, *J. Photogr. Sci.* **26** (1978), 242.

3. T. YANAGAWA AND I. TAKEKOSHI, *IEEE Trans. Electron. Devices* **17** (1970), 964.
4. C. VUIK, Report, Delft University of Technology, 1982.
5. J. R. OCKENDON AND W. R. HODGKINS, "Moving Boundary Problems in Heat Flow and Diffusion," Oxford Univ. Press (Clarendon), Oxford, 1975.
6. H. R. THIRSK AND J. A. HARRISON, "A guide to the Study of Electrode Kinetics," Academic Press, New York/London, 1972.
7. B. R. PAMPLIN, "Crystal Growth," Pergamon, Oxford, 1975.
8. C. W. CRYER, "A Survey of Trial Free Boundary Methods for the Numerical Solution of Free Boundary Problems," MRC Tech. Summ. Rep. 1693, 1976.
9. C. M. ELLIOTT AND J. R. OCKENDON, "Weak and Variational Methods for Moving Boundary Problems," Pitman, Boston, 1982.
10. A. FASANO AND M. PRIMICERIO, "Free Boundary Problems: Theory and Applications," Pitman, Boston, 1983.
11. J. L. LIONS, Introduction to some aspects of free surface problems, in "Numerical Solution of Partial Differential Equations" (B. Hubbard, Ed.), Academic Press, New York, 1976.
12. C. BAIOCCHI *et al.*, *Ann. Mat. Pura Appl.* **98** (1973), 1.
13. G. DUVAUT, *C. R. Acad. Sci. Paris* **276** (1973), 1461.
14. J. L. LIONS, "Quelques méthodes de résolution des problèmes aux limites non linéaires," Dunod, Paris, 1969.
15. R. GLOWINSKI, J. L. LIONS, AND R. TRÉMOLIÈRES, "Numerical Analysis of Variational Inequalities," North-Holland, Amsterdam, 1980.
16. C. W. CRYER, *SIAM J. Control* **9** (1971), 385.
17. R. S. VARGA, "Matrix Iterative Analysis," Prentice-Hall, London, 1962.
18. B. A. CARRÉ, *Comput. J.* **4** (1961), 73.
19. W. D. MURRAY AND F. LANDIS, *Trans. ASME J. Heat Transfer* **81** (1959), 106.
20. V. R. B. SANTOS, *Comp. Methods Appl. Mech. Eng.* **25** (1981), 51.
21. D. R. LYNCH, K. O'NEILL, *Int. J. Numer. Methods Eng.* **17** (1981), 81.
22. I. BABUSKA, A. K. AZIZ, *SIAM J. Numer. Anal.* **13** (1976), 214.
23. R. BONNEROT, AND P. JAMET, *J. Comput. Phys.* **25** (1977), 163.
24. H. K. KUIKEN, *Proc. Roy. Soc. London. Ser. A* **39b** (1984), 95.